Journal of Materials Chemistry

RSC Publishing

Journals Journal of Materials Chemistry Advance Articles DOI: 10.1039/b700505a

J. Mater. Chem., 2007 | DOI: 10.1039/b700505a | Communication

Observation of intermediate-range order in a nominally amorphous molecular semiconductor film

Daniel R. Blasini†[ab], Jonathan Rivnay†[c], Detlef-M. Smilgies*[b], Jason D. Slinker[c], Samuel Flores-Torres[a], Héctor D. Abruña[a] and George G. Malliaras[c]

[a]*Department of Chemistry and Chemical Biology, Cornell University, Ithaca, NY 14853, USA*

[b]*Cornell High-Energy Synchrotron Source (CHESS), Ithaca, NY 14853, USA. E-mail: dms79@cornell.edu; Fax: +1 607 255 9001; Tel: +1 607 255 0917*

[c]*Department of Materials Science and Engineering, Cornell University, Ithaca, NY 14853, USA*

Received 12th January 2007, Accepted 13th February 2007

First published on the web 20th February 2007

Synchrotron X-ray diffraction from a nominally amorphous molecular semiconductor film reveals both the presence of intermediate-range order (IRO) corresponding to crystalline domains with an average size of a few nanometres, and the growth of these domains upon exposure of the film to moisture.

Due to a high demand for better, more efficient, and less expensive displays and lighting, the science and engineering community has concentrated efforts on the development, understanding and optimization of new electroluminescent materials. Consequently, organic light emitting devices (OLEDs) have gained interest as an alternative to inorganic semiconductor technology.[1,2] Not surprisingly, device performance is strongly correlated to the microstructure of the organic thin films. While perfect single-crystalline films promise the best transport properties and quantum efficiencies, they are very difficult to deposit over large areas. Amorphous films have been found to perform significantly better than most polycrystalline films. The high surface roughness associated with the latter is problematic in sandwich-type structures. Moreover, grain boundaries in polycrystalline materials may provide trapping and recombination centres, which can degrade device performance and lifetime. In contrast, the hopping-type conductivity in amorphous films is adequate for several applications, including OLEDs and organic photovoltaics.[1] As a result, the development of amorphous molecular materials is of great interest.[3]

Changes in the film structure that occur during device operation are also of interest, as the structural integrity of the film affects device performance. Recrystallization of an amorphous film, for example, may lead to cracking or delamination, with catastrophic consequences for the device.[4,5] Understanding the local structure of amorphous films of organic semiconductors, and its evolution with device operation, is of fundamental importance to organic electronics. Unfortunately, very little is known about the local structure in such amorphous films. This is due to the fact that amorphous materials are relatively poor scatterers, so that standard X-ray scattering from thin films is very hard to obtain with lab-based X-ray generators. Furthermore, in device-relevant configurations, where the film thickness is of the order of 100 nm, scattering from the substrate can be pronounced and can obscure the faint scattering signatures from the film itself. Both problems can be overcome using synchrotron-based grazing incidence scattering methods, as we will demonstrate below. In this communication we investigate the microstructure of the ruthenium complex $[Ru(bpy)_3]^{2+}(PF_6^-)_2$, where bpy is 2,2′-bipyridine. This material and its analogues have recently attracted a great deal of attention as they allow the fabrication of high efficiency electroluminescent devices with air-stable electrodes.[6–19] We find that these films show intermediate-range order, exhibiting crystalline domains with an average size of a few nanometres. Moreover, these crystalline domains grow larger upon exposure of the films to moisture. These results suggest that a considerable degree of order can exist in molecular films thought to be amorphous. They also show that synchrotron-based X-ray diffraction is an extremely powerful tool in the development of amorphous materials for organic electronics.

Details on the synthesis of $[Ru(bpy)_3]^{2+}(PF_6^-)_2$ have been reported elsewhere.[12] Films were deposited by spin coating from solution consisting of 24 mg $[Ru(bpy)_3]^{2+}(PF_6^-)_2$ per mL of acetonitrile on indium tin oxide (ITO) coated glass slides (Thin Film Devices, Anaheim, CA). The deposition was performed inside a glove box with a dry nitrogen atmosphere. All films were approximately 100 nm thick and they were baked on a hot plate (inside the glove box) at 120 °C for 15 hours. To study the effect of moisture on film structure, some of the films were placed in a vacuum chamber. The latter was subsequently filled with a mixture of dry and wet nitrogen, exposing the films to various degrees of relative humidity (RH) over a period of 20 min. After fabrication/exposure, all samples were held under dry nitrogen until X-ray characterization.

X-Ray diffraction measurements were performed at the G2 beamline of the Cornell High-Energy Synchrotron Source (CHESS). An intense photon beam from the G-line 50-pole wiggler was monochromatised with W : B_4C multilayers (bandwidth about 1.5%) and mirrors. An X-ray transparent Be(0002) monochromator crystal deflected about 5% of the incident high-flux beam into the G2 side station. The basal plane mosaicity of the Be crystal of 0.03° yielded a photon energy bandwidth of 0.1% of the side-bounce X-ray

beam. The G2 grazing-incidence reciprocal space mapping system consists of a six-circle kappa diffractometer with a Soller collimator and a linear gas detector mounted vertically on the detector arm.[20] The linear gas detector and the Soller collimator have matching apertures of 8 mm width and 100 mm height with a horizontal resolution of 0.2° and a vertical resolution of 200 μm along the counting wire (equivalent to a 0.1° vertical resolution). The samples were mounted horizontally on a motorized height stage and the incident angle was controlled with the η motion of the diffractometer. The samples were illuminated by an X-ray beam of 5 mm width and 0.2 mm height, as defined by two sets of collimating slits in the incident X-ray beam. In order to reduce air scattering, control exposure to the ambient, and prevent radiation-induced oxidation of the organic materials,[21] the samples were kept in a helium-filled shroud with polyester (Mylar) windows.

The grazing-incidence scattering geometry was applied to enhance the weak thin film scattering signal over the diffuse scattering from the substrate. The incident angle π was chosen to be well below the ITO critical angle of about 0.3°, in order to reduce the intensity of the very strong ITO powder ring which overwhelms the faint and broad scattering features of the organic film. Fig. 1 shows this effect clearly by contrasting scattering maps at two incident angles: α = 0.13° (A), which is just above the critical angle of the film but well below the ITO critical angle, and α = 0.40° (B), which is just above the ITO critical angle. In the case of (B) the scattering signal is dominated by intense scattering from the ITO electrode, while the faint scattering of the $[Ru(bpy)_3]^{2+}(PF_6^-)_2$ film can hardly be discerned. By reducing the incident angle below the ITO critical angle and thus the X-ray penetration depth, the faint $[Ru(bpy)_3]^{2+}(PF_6^-)_2$ powder rings become clearly visible (A).

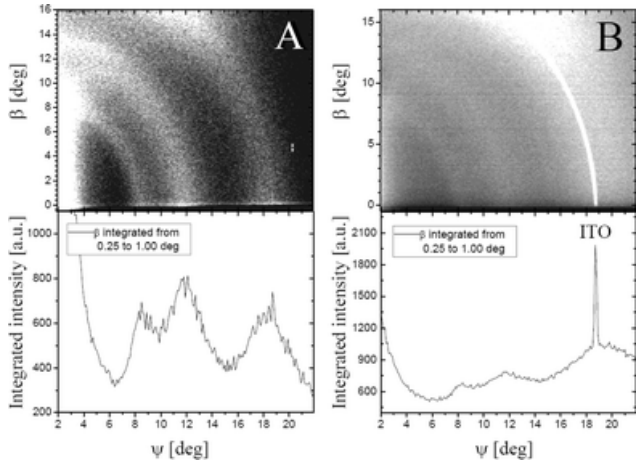

Fig. 1 Grazing incident diffraction from a $[Ru(bpy)_3]^{2+}(PF_6^-)_2$ film. Data were collected at an incident angle π = 0.13° (A), which is just above the critical angle of the film but below the ITO critical angle, and at α = 0.40° (B), which is just above the ITO critical angle. Below the scattering maps, scans of the intensity integrated from 0.25° < β < 1° are shown. λ = 1.34 Å.

Powder spectra were extracted from the scattering maps by integrating over a 0.75° exit angle (β) range (from 0.25° to 1°). These were compared to simulated spectra based on the single crystalline structure of $[Ru(bpy)_3]^{2+}(PF_6^-)_2$ using the programs CrystalMaker© and CrystalDiffract©. $[Ru(bpy)_3]^{2+}(PF_6^-)_2$ crystallizes in a trigonal lattice with space group No. 165 and lattice parameters $a = b$ = 10.76 Å, c = 16.36 Å, γ =120°.[22] Fig. 2 shows the results of these simulations. In the initial calculation (Fig. 2, curve d), the resolution-limited powder spectrum was simulated using the resolution of our set-up. In comparison, the measured powder spectrum (curve a) was significantly broadened, which is a telling sign of the formation of very small crystallites in the film. An average domain size of 3.3 nm reproduced our data (curve c). In a final step, the simulated spectrum was scaled (curve b) in order to obtain a reasonable fit of the peak positions to the experimental spectrum. This change corresponds to a lattice expansion of 7.8% in the crystallites. This expansion may be due to a modified solvent content in the film as compared to the single crystal,[23] or might be an intrinsic property of the nanoscale crystallites, as nanoparticles often feature somewhat expanded lattices.

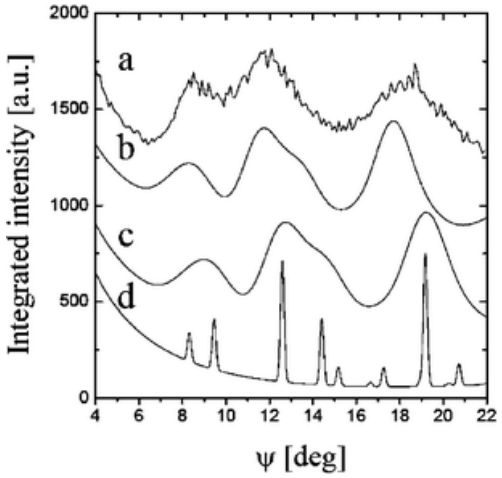

Fig. 2 Measured and simulated powder diffraction patterns. The measured curve (a) was extracted from the reciprocal space map shown in Fig. 1(A). Curve (c) is a simulation for an average crystallite size of 3.3 nm. Curve (b) shows the same powder spectrum, but with the lattice expanded by 7.8%. For comparison, curve (d) shows a simulated resolution-limited powder spectrum, based on the single-crystal structure.

Comparing the average crystallite size of about 33 Å to the measured expanded lattice constants of 11.6 Å, we see that crystallites with an average size of about 3 lattice constants formed. This amount of order is surprising, and to our knowledge it has not been observed before. Previous TEM studies have shown no order in these films down to 5 nm,[7] so these films have been thought to be amorphous. Amorphous structures as found in glasses are characterized by short-range order, *i.e.* only a nearest neighbour structure.[24] However, recently the importance of intermediate-range order (IRO) has been suggested in classic glassy materials,[25,26] and at this point it is not known whether IRO is a feature of the amorphous state or characterizes a different state of matter.[26]

Exposure to moisture was found to have a major influence on the structure of the films. Scattering maps from $[Ru(bpy)_3]^{2+}(PF_6^-)_2$ films exposed to different amounts of relative humidity (RH, Fig. 3) indicate a dramatic change in the order within these films. These experiments were performed at an incident angle of 0.25°—still below the total external reflection of ITO. Powder spectra extracted by integrating the intensity from $0.25° < \beta < 1°$ were compared to simulated ones, as before, to obtain estimates of average particle sizes and lattice expansions. Simulations along with experimental X-ray scattering data are shown in Fig. 4. The emergence of well-defined powder diffraction rings is evident in the film exposed to 20% RH. The data are consistent with an average crystallite size of 10 nm, and a slightly less expanded lattice (compared to the pristine films) of 2.1%. The film exposed to 44% humidity shows crystallites of 21 nm average size, and the same lattice expansion of 2.1%.

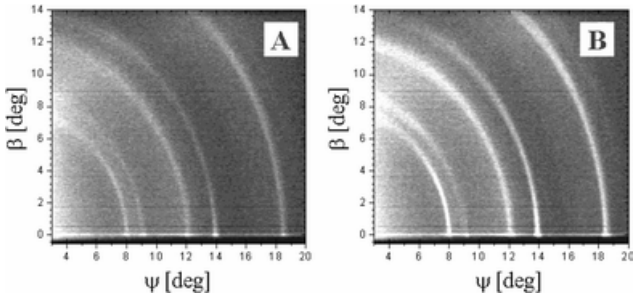

Fig. 3 Scattering maps from two $[Ru(bpy)_3]^{2+}(PF_6^-)_2$ films exposed to 20% RH (A) and to 44% RH (B), for ~20 min. λ = 1.32Å and α = 0.25°.

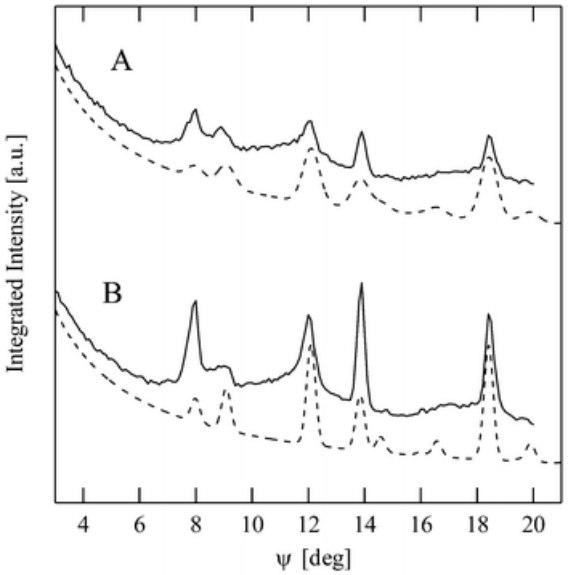

Fig. 4 Measured (solid) and simulated (dashed) diffraction patterns from films exposed to 20% RH (A) and 44% (B).

The growth of the crystalline domains in the film is evident within the relative humidity range studied. Whereas the IRO found in the non-treated films is characterized by crystallites with an average size of about 3 lattice constants, the samples exposed to moisture show a higher degree of order. The crystalline domains have average sizes of 9 and 19 lattice constants for films exposed to 20% RH and 44% RH, respectively. The larger crystalline domains at higher humidity show that water assists in ordering the $[Ru(bpy)_3]^{2+}(PF_6^-)_2$ film.

Exposure to moisture is known to degrade the performance of $[Ru(bpy)_3]^{2+}(PF_6^-)_2$ electroluminescent devices.[27–30] This has been linked to the formation of quenchers, such as an oxo-bridged dimer,[29,30] during device operation in ambient. At this point, it is not clear whether the structural evolution of the $[Ru(bpy)_3]^{2+}(PF_6^-)_2$ films upon exposure to moisture plays a significant role in device degradation. However, this work implies that in addition to chemical degradation, "structural degradation" might also be important.

In conclusion, we report the presence of IRO in thin films of the molecular semiconductor $[Ru(bpy)_3]^{2+}(PF_6^-)_2$. Exposure to moisture increases order in the films. Grazing incidence synchrotron X-ray diffraction is shown to be an extremely powerful tool for probing the structures of device-grade organic semiconductor films that are nominally amorphous. Using this technique to characterize the presence and evolution of structure in families of analogous molecules is expected to play a key role in discovering organic semiconductors with improved robustness towards crystallization.

Acknowledgements

This work was supported by NYSTAR and the NSF through the Cornell Center of Materials Research (CCMR). The G2 station and the reciprocal space mapping system was funded by NSF as well as by the CCMR and Cornell University. Special thanks to Dave Nowak (Cornell) and Basil Blank (Spacemill Industries). DRB and JDS were supported by an NSF Graduate Research Fellowship. CHESS is a national user facility supported by the NSF award DMR-0225180.

Notes and references

1 G. G. Malliaras and R. H. Friend, *Phys. Today*, 2005, **58**, 53 [Links].
2 A. Bergh, G. Craford, A. Duggal and R. Haitz, *Phys. Today*, 2001, **54**, 42 [Links].
3 Y. Shirota, *J. Mater. Chem.*, 2005, **15**, 75 [Links].
4 L. Do, E. Han, N. Yamamoto and M. Fujihira, *Mol. Cryst. Liq. Cryst.*, 1996, **280**, 373 [Links].
5 H. Aziz, Z. Popovic, S. Xie, A.-M. Hor, N.-X. Hu, C. Tripp and G. Xu, *Appl. Phys. Lett.*, 1998, **72**, 756 [Links].
6 E. S. Handy, A. J. Pal and M. F. Rubner, *J. Am. Chem. Soc.*, 1999, **121**, 3525 [Links].
7 F. G. Gao and A. J. Bard, *J. Am. Chem. Soc.*, 2000, **122**, 7426 [Links].
8 H. Rudmann and M. F. Rubner, *J. Appl. Phys.*, 2001, **90**, 4338 [Links].
9 S. Bernhard, X. Gao, G. G. Malliaras and H. D. Abruña, *Adv. Mater.*, 2002, **14**, 433 [Links].
10 H. Rudmann, S. Shimada and M. F. Rubner, *J. Am. Chem. Soc.*, 2002, **124**, 4918 [Links].
11 M. Buda, G. Kalyuzhny and A. J. Bard, *J. Am. Chem. Soc.*, 2002, **124**, 6090 [Links].
12 S. Bernhard, J. A. Barron, P. L. Houston, H. D. Abruña, J. L. Ruglovksy, X. Gao and G. G. Malliaras, *J. Am. Chem. Soc.*, 2002, **124**, 13624 [Links].

13 J. Slinker, D. Bernards, P. L. Houston, H. D. Abruña, S. Bernhard and G. G. Malliaras, *Chem. Commun.*, 2003, 2392 [Links].

14 J. D. Slinker, A. A. Gorodetsky, M. S. Lowry, J. Wang, S. Parker, R. Rohl, S. Bernhard and G. G. Malliaras, *J. Am. Chem. Soc.*, 2004, **126**, 2763 [Links].

15 A. B. Tamayo, S. Garon, T. Sajoto, P. I. Djurovich, I. M. Tsyba, R. Bau and M. E. Thompson, *Inorg. Chem.*, 2005, **44**, 8723 [Links].

16 E. H. Holder, B. M. W. Langeveld and U. S. Schubert, *Adv. Mater.*, 2005, **17**, 1109 [Links].

17 H. J. Bolink, L. Cappelli, E. Coronado, M. Grätzel and M. K. Nazeeruddin, *J. Am. Chem. Soc.*, 2006, **128**, 46 [Links].

18 H. J. Bolink, L. Cappelli, E. Coronado, A. Parham and P. Stössel, *Chem. Mater.*, 2006, **18**, 2778 [Links].

19 D. A. Bernards, S. Flores-Torres, H. D. Abruña and G. G. Malliaras, *Science*, 2006, **313**, 1416 [Links].

20 D.-M. Smilgies, D. R. Blasini, S. Hotta and H. Yanagi, *J. Synchrotron Radiat.*, 2005, **12**, 807 [Links].

21 D.-M. Smilgies, N. Boudet and H. Yanagi, *Appl. Surf. Sci.*, 2002, **189**, 24 [Links].

22 D. P. Rillema, D. S. Jones, C. Woods and H. A. Levy, *Inorg. Chem.*, 1992, **31**, 2935 [Links].

23 W. Zhao, C.-Y. Liu, Q. Wang, J. M. White and A. J. Bard, *Chem. Mater.*, 2005, **17**, 6403 [Links].

24 R. L. Mozzi and B. E. Warren, *J. Appl. Crystallogr.*, 1969, **2**, 164 [Links].

25 J. D. Martin, S. J. Goettler, N. Fosse and L. Iton, *Nature*, 2002, **419**, 381 [Links].

26 T. C. Hufnagel, *Nat. Mater.*, 2004, **3**, 666 [Links].

27 G. Kalyuzhny, M. Buda, J. McNeill, P. Barbara and A. J. Bard, *J. Am. Chem. Soc.*, 2003, **125**, 6272 [Links].

28 D. L. Pile and A. J. Bard, *Chem. Mater.*, 2005, **17**, 4212 [Links].

29 L. Soltzberg, J. D. Slinker, S. Flores-Torres, D. A. Bernards, G. G. Malliaras, H. D. Abruña, J.-S. Kim, R. H. Friend, M. D. Kaplan and V. Goldberg, *J. Am. Chem. Soc.*, 2006, **128**, 7761 [Links].

30 J. D. Slinker, J.-S. Kim, S. Flores-Torres, J. H. Delcamp, H. D. Abruña, R. H. Friend and G. G. Malliaras, *J. Mater. Chem.*, 2007, **17**, 76 [Links].

Footnote

† These authors contributed equally to this work.